Journal of the European Ceramic Society 22 (2002) 579–583

www.elsevier.com/locate/jeurceramsoc

The influence of grain boundary impedances on the p-type conductivity of undoped $BaTiO_3$ ceramics

I.J. Clark[a], F.B. Marques[b], D.C. Sinclair[a,*]

[a]*Department of Engineering Materials, Sir Robert Hadfield Building, University of Sheffield, Mappin Street, Sheffield S1 3JD, UK*
[b]*Department of Ceramics and Glass Engineering, UIMC, University of Aveiro, 3810 Averio, Portugal*

Received 15 December 2000; received in revised form 4 April 2001; accepted 28 April 2001

Abstract

Impedance spectroscopy is used to deconvolute the dc conductivity (σ) of undoped $BaTiO_3$ ceramics ($\sim$95% of the theoretical X-ray density) into bulk (σ_b) and grain boundary (σ_{gb}) components at two oxygen partial pressures, P_{O_2} $\sim$10 Pa (N_2) and $\sim$0.21 MPa (air). At 900°C, $\sigma \sim \sigma_b$ in both atmospheres, however, at lower temperatures Z^* plots are dominated by the grain boundary component and $\sigma \sim \sigma_{gb}$. The temperature of the switch from $\sigma \sim \sigma_b$ to $\sigma \sim \sigma_{gb}$ is different in the two atmospheres and occurs at $\sim$850°C in air and $\sim$650°C in N_2. Isothermal plots of log σ_b vs log P_{O_2} in the temperature range 450–900°C show the expected oxygen partial pressure dependence with a gradient of $+1/4$. In contrast, σ_{gb} is relatively insensitive to P_{O_2} and log σ_{gb} vs log P_{O_2} plots have gradients $< +1/4$ with values as low as $\sim +1/14.0$. In general, isothermal log σ vs log pO_2 plots have gradients $< +1/4$ as σ is dominated by the grain boundary component. This may explain the wide range of gradients ($\sim$1/4–1/9) reported in the literature for isothermal dc conductivity measurements on polycrystalline $BaTiO_3$ in the p-type regime.

Keywords: $BaTiO_3$; Electrical conductivity; Electrical properties; Grain boundaries; Impedance spectroscopy

1. Introduction

The defect chemistry of undoped $BaTiO_3$ is commonly investigated by measuring the oxygen partial pressure, P_{O_2}, dependence of the electrical conductivity, σ, at temperatures $>$ 750°C. A schematic log σ vs log P_{O_2} plot for undoped $BaTiO_3$ ceramics below $\sim$1000°C where σ is p-type in the range $\sim 10^{-1}$–10^5 Pa and n-type below $\sim 10^{-1}$Pa is shown in Fig. 1.[1,2] The conductivity minimum at $P^0_{O_2}$, which separates the p- and n-type regions, shifts to higher P_{O_2} with increasing temperature and corresponds to the intrinsic conductivity associated with direct ionisation of charge carriers across the band gap.

Chan et al.[1,2] have modelled the conductivity behaviour of undoped $BaTiO_3$ ceramics in terms of the so-called 'extrinsic' model, where the unexpected p-type behaviour below $\sim$1000°C and $P_{O_2} > 10^{-1}$ Pa is attributed to the presence of unavoidable aliovalent impurities such as Fe and Al on the Ti-sites of the $BaTiO_3$ lattice. These aliovalent impurities, present at low levels (10′s of parts per million) in high purity reagent grade TiO_2, produce oxygen vacancies within the $BaTiO_3$ lattice and provide an easy mechanism to account for the observed p-type behaviour, viz

$$V_O^{\bullet\bullet} + 1/2O_2 => O_O^x + 2h^{\bullet} \quad (1)$$

where $V_O^{\bullet\bullet}$, O_O^x and $h^{\bullet}$ represent oxygen vacancies, oxygen ions in the lattice and electron holes, respectively.

Based on this model, log σ vs log P_{O_2} plots should have a gradient, $1/m$ (where m = exponent), of $+1/4$ in the p-type region, however, a large spread of m values, ranging from $+3.45$ to $+9.09$ have been reported for temperatures between 700 and 1200°C.[3–7] It is noteworthy that a low slope in such plots corresponds to a high value of m. Several experimental factors limit the data range for the p-type region. For example, sample-atmosphere equilibration times are lengthy for temperatures below $\sim$700°C and, therefore, most groups only report data for temperatures above $\sim$750°C. Conductivity measurements are rarely performed at P_{O_2} $> 10^5$ Pa, thus restricting the P_{O_2} range for the p-type region between 10^0–10^5 Pa. In addition, the switch from

* Corresponding author.
E-mail address: d.c.sinclair@sheffield.ac.uk (D.C. Sinclair).

0955-2219/02/$ - see front matter
PII: S0955-2219(01)00314-4

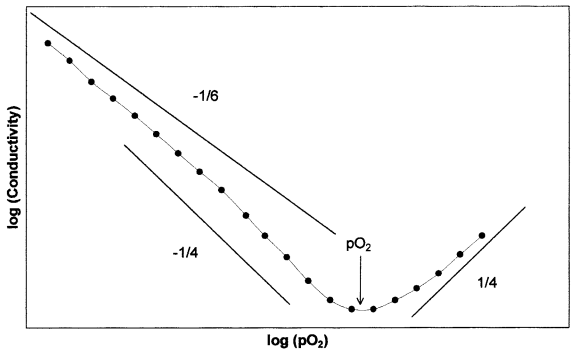

Fig. 1. A schematic plot of log σ vs log P_{O_2} for undoped $BaTiO_3$ at $\geqslant$ 750°C.

n- to p-type behaviour at $P^0_{O_2}$ occurs over a broad P_{O_2} range which moves to higher P_{O_2} with increasing temperature. This latter effect makes the process of defining the P_{O_2} range to calculate m for the p-type region a rather arbitrary process, especially at high temperatures.

ac Impedance spectroscopy, IS, on polycrystalline $BaTiO_3$ has shown the pellet resistance R_T above the ferroelectric Curie temperature at ~130°C to be a summation of intra- and intergranular resistances, R_b and R_{gb}, respectively, viz.

$$R_T = R_b + R_{gb} \tag{2}$$

Such ceramics are commonly modelled on an equivalent circuit consisting of two parallel resistor-capacitor (RC) elements connected in series (Fig. 2). The RC elements represent intra- and intergranular regions of the ceramic, respectively and each gives rise to a semicircular arc in complex impedance plane, Z^*, plots. To our knowledge, the P_{O_2} dependence of R_{gb} in undoped $BaTiO_3$ ceramics has not been reported, and, therefore, nor has its influence on σ as

$$\sigma = (L/A).R_T^{-1} = (L/A).\left(R_b + R_{gb}\right)^{-1} \tag{3}$$

where L is the pellet thickness and A is the cross-sectional electrode area. Based on Eq. (3), differences in σ for high purity single crystal and polycrystalline samples will depend on the magnitude of R_{gb}.

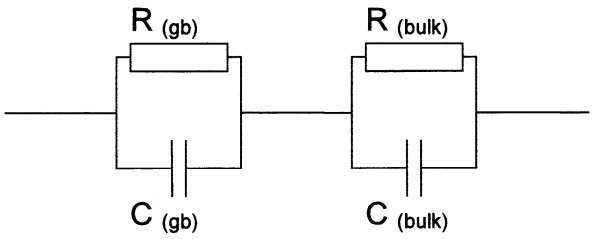

Fig. 2. Equivalent circuit used to model the electrical behaviour of undoped $BaTiO_3$ ceramics above the ferroelectric Curie temperature.

As far as we are aware, most σ vs P_{O_2} studies on polycrystalline $BaTiO_3$ of ceramics have ignored R_{gb} as measurements are traditionally performed at elevated temperatures (>700°C) where $R_b >> R_{gb}$ is assumed and, therefore, Eq. (3) is simplified to

$$\sigma \equiv (L/A).R_b^{-1} = \sigma_b \tag{4}$$

where σ_b is the bulk conductivity. Experimental results verify the use of Eq. (4) for data on ceramics in the n-type region however, large discrepancies between data for single crystals and ceramics are observed in the p-type region.[8] In this paper we use IS to separate σ into bulk and grain boundary components for undoped $BaTiO_3$ ceramics equilibrated in N_2 (P_{O_2} ~10^1 Pa) and air (P_{O_2} ~0.21×10^5 Pa) and discuss the influence of R_{gb} on σ in the p-type region.

2. Experimental

$BaTiO_3$ powder was prepared by hydrothermal reaction of $TiO_2{\cdot}H_2O$ (>99%, Mitsuwa Chemicals) and $Ba(OH)_2{\cdot}8H_2O$ (98%+, Aldrich) at 180°C for 72 h as described previously.[9] A Hagg–Guinier camera using Cu $K_{\alpha1}$ radiation was used to determine the purity of the powders. As-prepared powder was then wet milled with (0.3 wt.%) PVA binder, dried at 200°C and pressed into pellets (10 mm diameter×2 mm thick) under a pressure of 500 MPa. Green compacts were fired at 1350°C for 16 h and the density of resulting pellets was determined by the Archimedes method. For impedance analysis, pellets were coated on both faces with platinum paste and fired in air at 800°C to remove all volatiles from the organo-paste thus forming hardened metal electrodes. Samples were then mounted in an impedance jig with an oxygen sensor and a type-B thermocouple and inserted in a tube furnace operating between ca. 400 and 1000°C. The P_{O_2} rig set-up has been described previously:[10] it allowed the sample temperature to be measured to ±1°C and the P_{O_2} of the N_2 atmosphere to be measured at each temperature.

Impedance measurements were performed in air and N_2 between 400 and 1000°C across the frequency range 20 Hz–1 MHz using an HP4192 impedance analyser with an applied voltage of 100 mV. On changing the atmosphere from air to N_2, or vice-versa, the sample was equilibrated at 1000°C. After equilibrium had been attained at 1000°C (ca. 12–15 h), measurements were performed down to ca. 400°C in steps of ~50°C. Permittivity versus temperature plots were constructed from IS data measured in air between 25 and 500°C across the frequency range 0.1 Hz–1 MHz using a Solartron 1260 Gain Phase Analyser coupled to a Solartron 1296 Dielectric Interface with an applied voltage of 100 mV.

3. Results and discussion

$BaTiO_3$ pellets were off-white in appearance, phase pure by X-ray diffraction and ~95% dense (compared to the theoretical X-ray density) with an average grain size of ~5 μm. All samples were electrically insulating at room temperature with $\sigma << 10^{-7}$ S cm^{-1}. Bulk permittivity values were extracted from a combination of fixed frequency (100 kHz, <300°C) and M^* (>250°C) data, as described elsewhere.[11] The data showed a permittivity maximum of ~9000 (Fig. 3), when heated through the ferro- to para-electric phase transition temperature at ~130°C. Curie–Weiss analysis of bulk data gave a Curie temperature of 125.7±2.4°C and a Curie constant of $1.37\times10^5\pm1.21\times10^3$°C. These values are in good agreement with those expected and demonstrate the dielectric behaviour is consistent with that of dense, undoped $BaTiO_3$ ceramics.[11]

Z^* plots for pellets equilibrated in N_2 and air atmospheres between ~400 and 800°C consisted of two overlapping semicircular arcs, as shown in Fig. 4. Above 800°C, σ >0.01 S cm^{-1} and it was not possible to resolve any semicircular arcs within the measured frequency range. All Z^* plots were modelled on the equivalent circuit given in Fig. 2 and capacitance values were estimated using the relationship $\omega RC=1$ at arc maxima (where ω is the angular frequency and $\omega=2\pi f$ where f is the applied frequency). The low frequency arc had an associated capacitance of ~1 nF and was attributed to the grain boundary response, whereas the capacitance of the high frequency arc decreased with increasing temperature, in the range 50–100 pF and was attributed to the bulk (paraelectric) response. R_b and R_{gb} values were extracted from the individual arc diameters and R_T was estimated as the low frequency intercept of the impedance data on the real axis, Z'. σ_b, σ_{gb} and σ were obtained by taking the reciprocal of the respective R_b, R_{gb} and R_T values after being corrected for pellet geometry. The magnitude of σ_{gb} values calculated using this approach need to be treated with caution as the correct geometric factor for this component is unknown due to their irregular geometry. In the absence of an appropriate grain boundary geometric factor it was decided to correct all R values for pellet geometry to allow σ and σ_b values to be correlated with existing literature values.

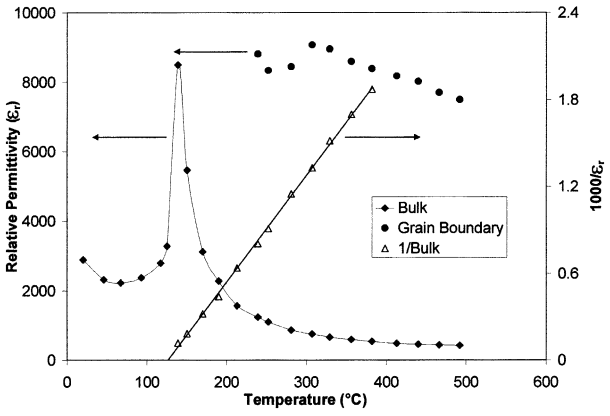

Fig. 3. Bulk (filled squares) and grain boundary (filled circles) permittivity data as a function of temperature. A Curie–Weiss plot of bulk data is shown by open triangles.

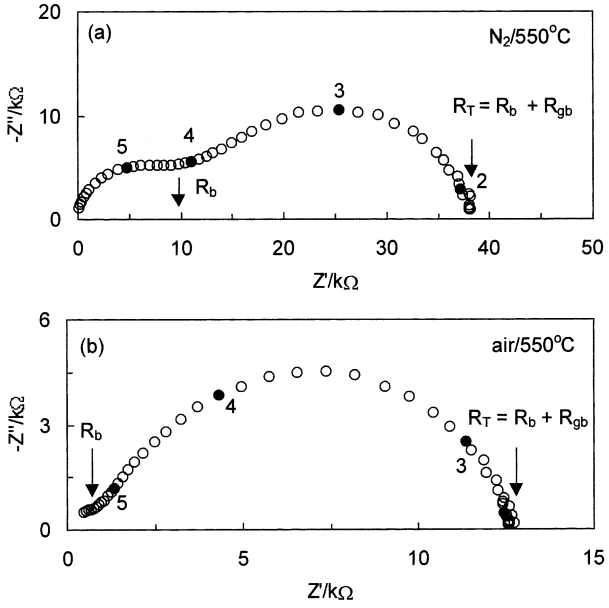

Fig. 4. Complex impedance plane plots measured in N_2 (a) and air (b), at 550°C. Selected frequencies (in Hz) are shown by filled circles on a log scale, e.g. $2=10^2$ Hz. Geometric factor (L/A) of pellet = 0.2 cm^{-1}.

Fig. 4 shows the relative contributions of R_b and R_{gb} to R_T at ~550°C in the different atmospheres. In N_2, R_b and R_{gb} have similar values, i.e. 10 and 28 kΩ respectively, both contribute significantly to R_T and, therefore, to σ [Eq. (3)]. In air, values of ~1 and 12 kΩ are observed for R_b and R_{gb}, respectively, $R_{gb}\sim R_T$ and, therefore, σ is dominated by σ_{gb} [Eq. (3)]. The ratio of $R_b(N_2)/R_b$(air) is 12:1 whereas $R_{gb}(N_2)/R_{gb}$(air) is 2.8:1 and highlights the greater sensitivity of the bulk response to changing P_{O_2} at this temperature.

σ_b, σ_{gb} And σ values from Z^* data for N_2 and air atmospheres are summarised in Arrhenius format for ~400–900°C, Fig. 5(a) and (b), respectively and, as expected for p-type behaviour, σ (air) > σ (N_2). The activation energies associated with the bulk and grain boundary conductivity are ~0.8 and 1.5 eV, respectively. To further aid comparison, Fig. 5(c) and (d) shows the temperature dependence of σ_b and σ_{gb} in N_2 and air, respectively. The bulk conductivity increases by ca. one order of magnitude on changing from N_2 to air at any given temperature [Fig. 5(c)], whereas the grain boundary conductivity is relatively insensitive to a similar change in P_{O_2} [Fig. 5(d)].

$\sigma_b >> \sigma_{gb}$ at low temperatures, ~400°C, in both atmospheres and, therefore, σ is dominated by σ_{gb},

however, σ_b is one order of magnitude greater in air than in N_2 (Fig. 5). As the temperature increases, the higher activation energy of σ_{gb} with respect to σ_b results in $\sigma_{gb} \sim \sigma_b$ at 650°C in N_2 and ~850°C in air. At high temperatures, ~900°C, $\sigma_b << \sigma_{gb}$ and σ is dominated by σ_b. The Arrhenius plot in Fig. 5(a) demonstrates σ (N_2) to be dominated by σ_{gb} below ~650°C (1000 K/T = 1.1) and that temperatures >700°C are required before $\sigma \sim \sigma_b$. Since σ_b increases by approximately one order of magnitude on increasing log (P_{O_2}/Pa) from 0.23 (N_2) to 4.32 (air), [Fig. 5(c)] whereas σ_{gb} is relatively insensitive to P_{O_2} [Fig. 5(d)], temperatures in excess of ~ 850°C (1000 K/T = 0.9) are required to ensure σ (air) ~ σ_b [Fig. 5(b)]. The "cross-over" temperature from $\sigma \sim \sigma_{gb}$ to $\sigma \sim \sigma_b$ occurs at different temperatures for N_2 and air atmospheres thus showing the condition where $\sigma = \sigma_b$ [Eq. (4)], to be dependent both on temperature and oxygen partial pressure. The IS results are conveniently summarised in Arrhenius format, Fig. 6 which shows the change in "cross-over" temperature for N_2 and air atmospheres. The assumption that $\sigma = \sigma_b$ [Eq. (4)] at > 700°C is, therefore, of limited use, especially in the high P_{O_2} region (i.e. air) where σ can be dominated by σ_{gb} up to ~850°C.

As an extreme example, Fig. 7(a) shows the deconvolution of σ at 600°C into bulk and grain boundary components, as measured in N_2 and air by IS. The bulk conductivity shows the expected behaviour with $m \sim +4.0$, in accordance with Eq. (1), whereas, the grain boundary conductivity shows very little P_{O_2}-dependence and has a much smaller slope with $m = +14.0$. As σ_{gb} dominates σ at 600°C (especially in air), σ also shows weak P_{O_2}-dependence with $m = +8.8$, a value significantly different to the expected +4 and that observed for the

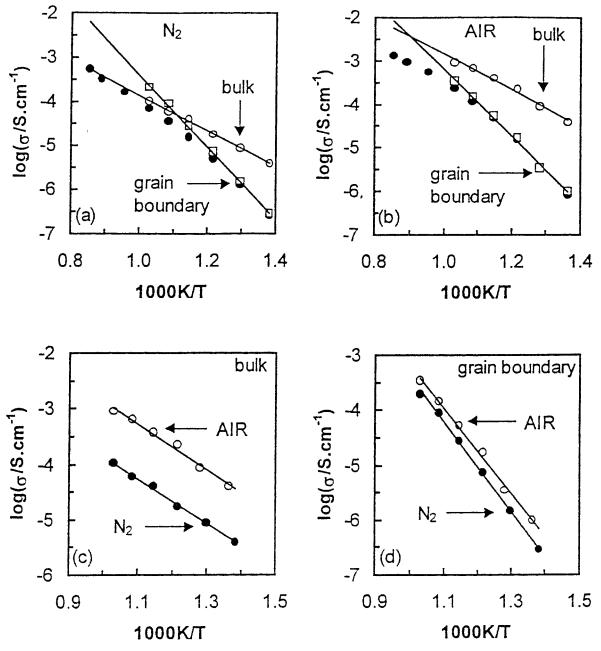

Fig. 5. Arrhenius plots of σ, σ_b and σ_{gb} in air (a), and N_2 (b), and of σ_b in air and N_2 (c) and σ_{gb} in air and N_2 (d).

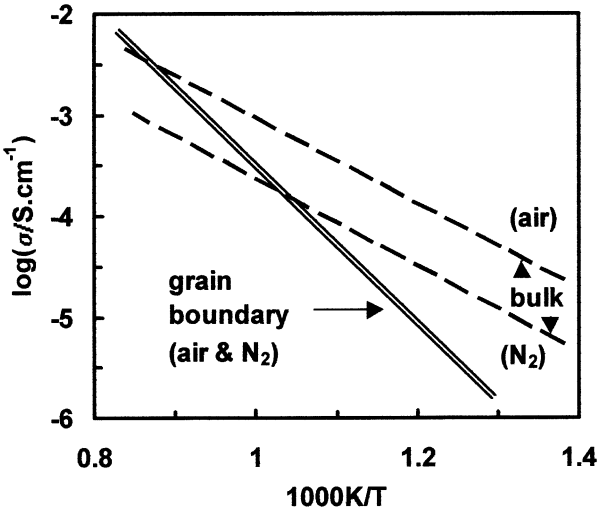

Fig. 6. Combined Arrhenius plots of σ_b and σ_{gb} in air and N_2 atmospheres.

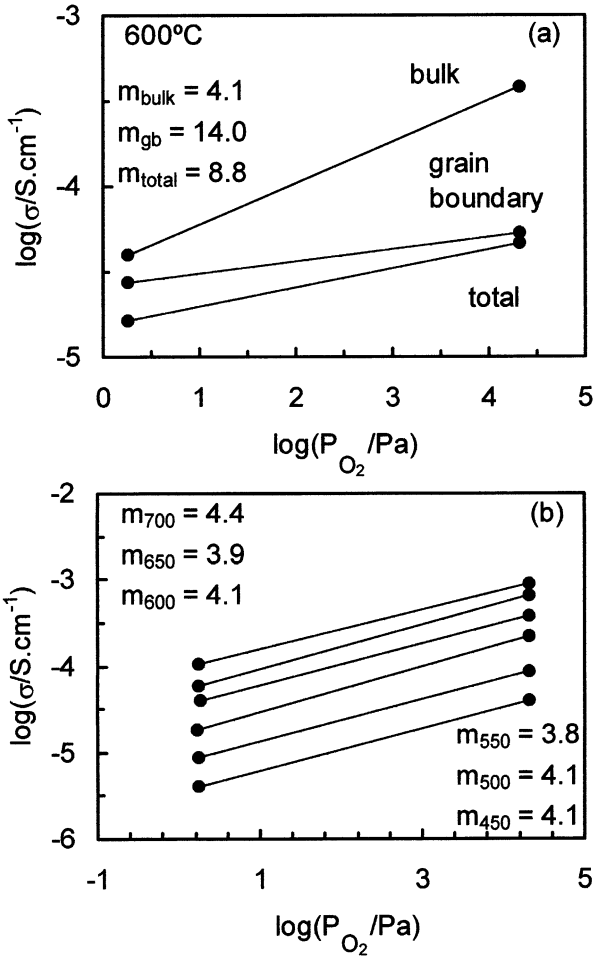

Fig. 7. Log σ vs log P_{O_2} plots for σ, σ_b and σ_{gb} in air and N_2 at 600°C (a) and log σ_b vs log P_{O_2} for temperatures 450–700°C, (b) $m = 1$/slope.

bulk conductivity behaviour. Grain boundary impedances can, therefore, give rise to erroneous m values in isothermal log σ vs log P_{O_2} plots of dc conductivity data in the p-type region.

σ_b Values at log P_{O_2} of 0.23 and 4.32 for $\sim$450–700°C are shown in Fig. 7(b) and demonstrate that m values of $\sim +4$ can be obtained below 700°C. The switch from p- to n-type behaviour occurs at log $P^0_{O_2} \sim -1$ for undoped $BaTiO_3$ at 700°C[1,2] and moves to lower P_{O_2} with decreasing temperature. All σ_b data in air and N_2 below 700°C can, therefore, be assumed to be unaffected by the broad conductivity minimum at $P^0_{O_2}$ (Fig. 1). The weak P_{O_2}-dependent σ behaviour observed below 700°C is attributed to the presence of large and P_{O_2}-insensitive grain boundary impedances in polycrystalline samples [Fig. 7(a)] as opposed to non-equilibrium effects with the gas ambient at these 'low' temperatures.

From our results we propose the wide range of m values >4 reported for polycrystalline $BaTiO_3$ at temperatures <1000°C is because σ from conventional dc measurements contains a significant contribution from the grain boundary regions. This proposal is difficult to prove conclusively as extracted m values are subject to large errors due to the "narrow window" of p-type behaviour coupled to the presence of the broad minimum at $P^0_{O_2}$, for temperatures >900°C. Samples are too conductive to obtain reliable IS data at >900°C and only dc values can be obtained. It should be emphasised that the reported "cross-over" temperatures where $\sigma_b \sim \sigma_{gb}$ in Fig. 6 are not 'universal' temperatures for undoped-$BaTiO_3$ ceramics in N_2 and air atmospheres. They are influenced by many factors including ceramic microstructure/pellet density and a more complete description of how the composition of the grain boundaries and microstructure influence log σ vs log P_{O_2} behaviour will be reported elsewhere.[12]

4. Conclusions

IS performed as a function of temperature in air and N_2 has been shown to overcome several limitations of isothermal dc conductivity measurements of undoped $BaTiO_3$ ceramics in the p-type region. Bulk and grain boundary components of σ can be obtained at temperatures as low as ca. 450°C and whereas the P_{O_2}-dependence of σ_b has the expected gradient with an m value of $+4$, σ_{gb} is relatively insensitive to P_{O_2} and has a much larger m value. Although $\sigma \sim \sigma_b$ in N_2 at >700°C, temperatures in excess of 850°C in air are required before $\sigma \sim \sigma_b$. This demonstrates the limitation of assuming $\sigma = \sigma_b$ at >700°C in isothermal dc conductivity measurements of undoped-$BaTiO_3$ ceramics in the p-type region, even for samples with $\sim$95% of the theoretical X-ray density. This may explain the large variation in m values reported in the literature for polycrystalline $BaTiO_3$ from isothermal dc conductivity measurements.

Acknowledgements

The authors would like to thank the EPSRC (studentship to I.J.C.), Erasmus and FTC (Portugal) for financial support during this research. D.C.S. would also like to thank The Royal Society of Chemistry for a J.W.T Jones Travel Fellowship.

References

1. Chan, N. H., Sharma, R. K. and Smyth, D. M., Non-stoichiometry in undoped barium titanate. *J. Am. Ceram. Soc.,* 1981, **64**(9), 556–562.
2. Chan, N. H., Sharma, R. K. and Smyth, D. M., Non-stoichiometry in acceptor doped barium titanate. *J. Am. Ceram. Soc.,* 1982, **65**(3), 167–170.
3. Daniels, J., Hardtl, K. H., Hennings, D. and Wernicke, R., Defect chemistry and electrical conductivity of doped barium titanate ceramics. *Philips Res. Repts.,* 1976, **31**, 487–559.
4. Seuter, A. M. J. G., Defect chemistry and electrical transport properties of barium titanate. *Philips Res. Repts. Suppl.*, 1974, **3**.
5. Long, S. A. and Blumenthal, R. N., Ti-rich non-stoichiometric $BaTiO_3$: I, high-temperature electrical conductivity measurements. *J. Am. Ceram. Soc.,* 1971, **54**(11), 515–519.
6. Eror, N. G. and Smyth, D. M., Non-stoichiometric disorder in single-crystalline $BaTiO_3$ at elevated temperatures. *J. Solid State Chem.,* 1978, **24**, 235–244.
7. Chan, N. H. and Smyth, D. M., Defect chemistry of donor doped $BaTiO_3$. *J. Am. Ceram. Soc.,* 1984, **67**(4), 285–288.
8. Nowotny, J. and Rekas, M., Defect chemistry of $BaTiO_3$. *Solid State Ionics,* 1991, **49**, 135–154.
9. Clark, I. J., Takeuchi, T., Ohtori, N. and Sinclair, D. C., Hydrothermal synthesis and characterisation of $BaTiO_3$ fine powders: precursors, polymorphism and properties. *J. Mater. Chem.,* 1999, **9**, 83–91.
10. Navarro, L. M., Marques, F. M. B. and Frade, J. R., N-type conduction in gadolinia doped ceria. *J. Electroceram. Soc.,* 1997, **144**, 267–273.
11. Hirose, N. and West, A. R., Impedance spectroscopy of undoped $BaTiO_3$. *J. Am. Ceram. Soc.,* 1996, **79**(6), 1633–1641.
12. Clark, I. J., PhD thesis. University of Sheffield, 2001.